



## **COMNAP Preliminary Research Report: Understanding Risk to National Antarctic Program Operations and Personnel in Coastal Antarctica from Tsunami Events**

version: July 2011

### **Abstract**

Even before the recent series of large magnitude earthquakes around the Pacific rim, there was concern expressed by National Antarctic Programs that we did not understand the risk to coastal Antarctic infrastructure and personnel in the event that tsunami waves reached coastal Antarctica. The recent series of large magnitude earthquakes has only added to that concern, since increased wave height was recorded on Antarctic tidal gauges after the recent earthquakes in Japan and New Zealand. This report aims to identify potential tsunami threats via modelling, so that Antarctic groups can make some assessment as to how vulnerable their infrastructure and operations are, and hence make informed decisions regarding future events. This will assist in planning in the future.

In November 2010, COMNAP EXCOM agreed to support a project on understanding tsunami risk. This paper presents the preliminary results of that project which was undertaken by a geology student from the University of Canterbury from the Natural Hazards Research Centre, Mr. Max Gallagher. The student was supervised and the project was overseen by two senior earth scientists, Dr. Thomas Wilson (Disasters and Hazards Management specialist, University of Canterbury) and Dr. Xiaoming Wang (Tsunami scientist and Tsunami modelling expert, GNS Crown Research Institute).

Ten tsunami models in total were produced using (an industry standard) the Cornell Multi-Grid Coupled Tsunami Model program (COMCOT v. 1.7). The models were run so as to originate from various tectonic boundaries around the Pacific Ocean in order to identify vulnerable regions along the Pacific section of the Antarctic coastline. Some of the models demonstrated that there is a risk to coastal Antarctic infrastructure, while others did not.

Modelling of the tsunamis use the linear approximation equations to calculate the volume fluxes, velocities fluxes and wave heights. The use of these equations means that shoaling or coastal amplification of the tsunami's wave height is not accounted for. Thus coastal regions will have higher wave amplitude than what is modelled here. Consequently, the tsunamis modelled here, are at the lower limit of what can theoretically be expected to occur.

Today, if an earthquake generated a tsunami similar to and originating from the same areas where the ten models were based, the tsunami would be detected by at least one tsunami buoy; however, that one buoy is not necessarily in between the tsunami's origin and the Antarctic destination. So there appears to be a lack of infrastructure for Antarctic early warning.

There is a general lack of tsunami buoys in the Antarctic region, Antarctica is usually left off of the tsunami warning maps and there is some opportunity for improvement in tsunami detection and

warning in the lower latitudes of the Pacific, especially given that the models demonstrate there is a risk to coastal Antarctic research stations. There is also a need for improved bathymetric data and for improved communications between relevant authorities and Antarctic base personnel. So that, in the event of tsunami approaching on coastal Antarctica, personnel can benefit from an early warning system that is accurate and effective. This preliminary study shows that further work is warranted and that there is a need for competent authorities to actively participant in this work.

## Background

Tsunamis may be generated by a number of different mechanisms; submarine landslide, bollide impact, volcanic events and tectonic uplift of the seafloor. The common component leading to tsunami formation is bulk water displacement occurring within a relatively short time frame. In this report, tectonic deformation of the sea floor is the only source considered as it is the most frequent cause of large tsunamis. Seafloor deformation producing tsunami is dominantly caused by the displacement on a fault interface at converging plate boundaries, associated with subduction zones. The subduction zones containing tsunami sources in this study are all situated along the Pacific Plate boundary, they are the South American, Aleutian, Kermadec and Puysegur subduction zones.

Since the Ross Sea Region, West Antarctica and the Antarctic Peninsula all effectively open to the Pacific Ocean, they are each potentially vulnerable to a large range of sources. There is thereby a need to model a variety of sources to try and identify what orientations of subduction segments will direct the generated tsunami wave at coastal regions in the Antarctic which currently support personnel and/or infrastructure. Therefore, the focus of this project was primarily the Peninsula Region (figure 1) and the Ross Sea Region (figure 2).

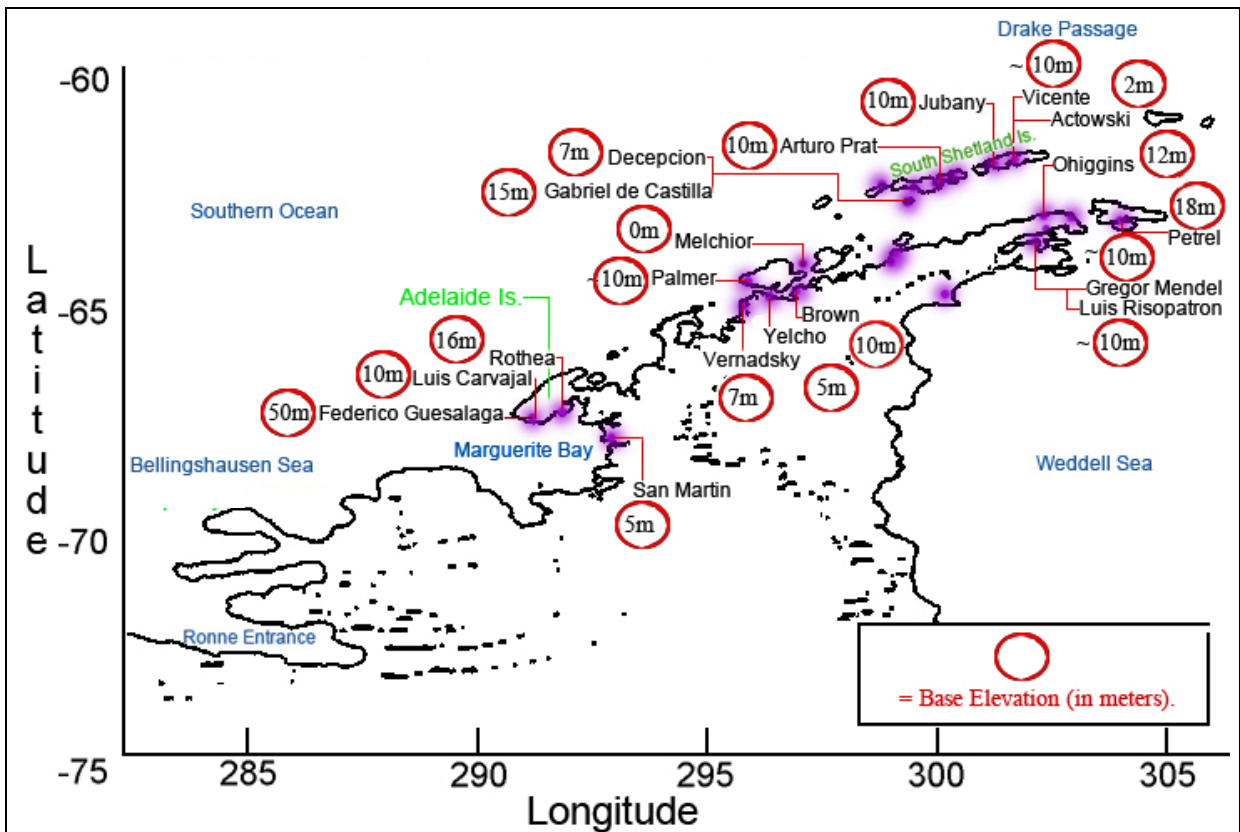


Figure 1: Antarctic research facilities in the Antarctic Peninsula. (Please note the map names are not from the CGA and they are not an endorsement of COMNAP in any way). Not all facilities are shown, some stations of high elevations or close proximity to already marked facilities have been left off this map.

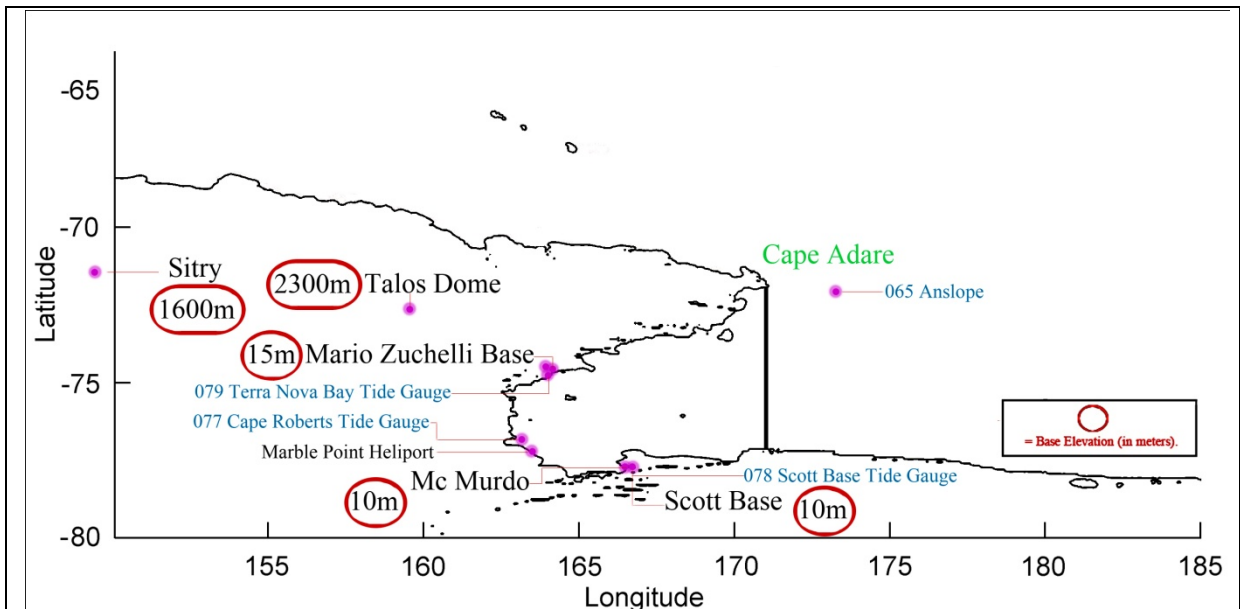


Figure 2: Antarctic research facilities of the Ross Sea Region. (Please note the map names are not from the CGA and they are not an endorsement of COMNAP in any way). Not all facilities are shown. This map also shows locations of tidal gauges.

There are many factors which have contributed to the fact that, in the past, the Antarctic region has literally been “left off the map” when it comes to tsunami modelling and tsunami hazard prediction. Current tsunami modelling, by organisations such as NOAA, is usually area specific, meaning that often such modelling rightfully focuses on areas of high coastal populations and cuts out areas of low or no population (see Satake 2007, as an example). There is a need to be selective in order to be efficient with respect to tsunami hazard evaluation. The computational time required by modelling software can mean that Antarctica is excluded from models which take time to process tsunami wave propagation to far-reaching places from the tsunami source. The larger models cover larger areas and hence require large bathymetry files that will affect the processing speed. Also, a desire to have higher resolution images of an area of interest, has led to cropping of the full model tsunami map. These factors have meant that Antarctica has, in the past, not been included in tsunami modelling.

For “real” events, tsunami detection via buoys is the prominent method of active detection. The tsunami buoy coverage for the Antarctic coastal region, however, is virtually non-existent (figure 3). Even buoys in the South Pacific are somewhat scarce and this limits the information available for communication of real-time tsunami threats to coastal Antarctic stations.

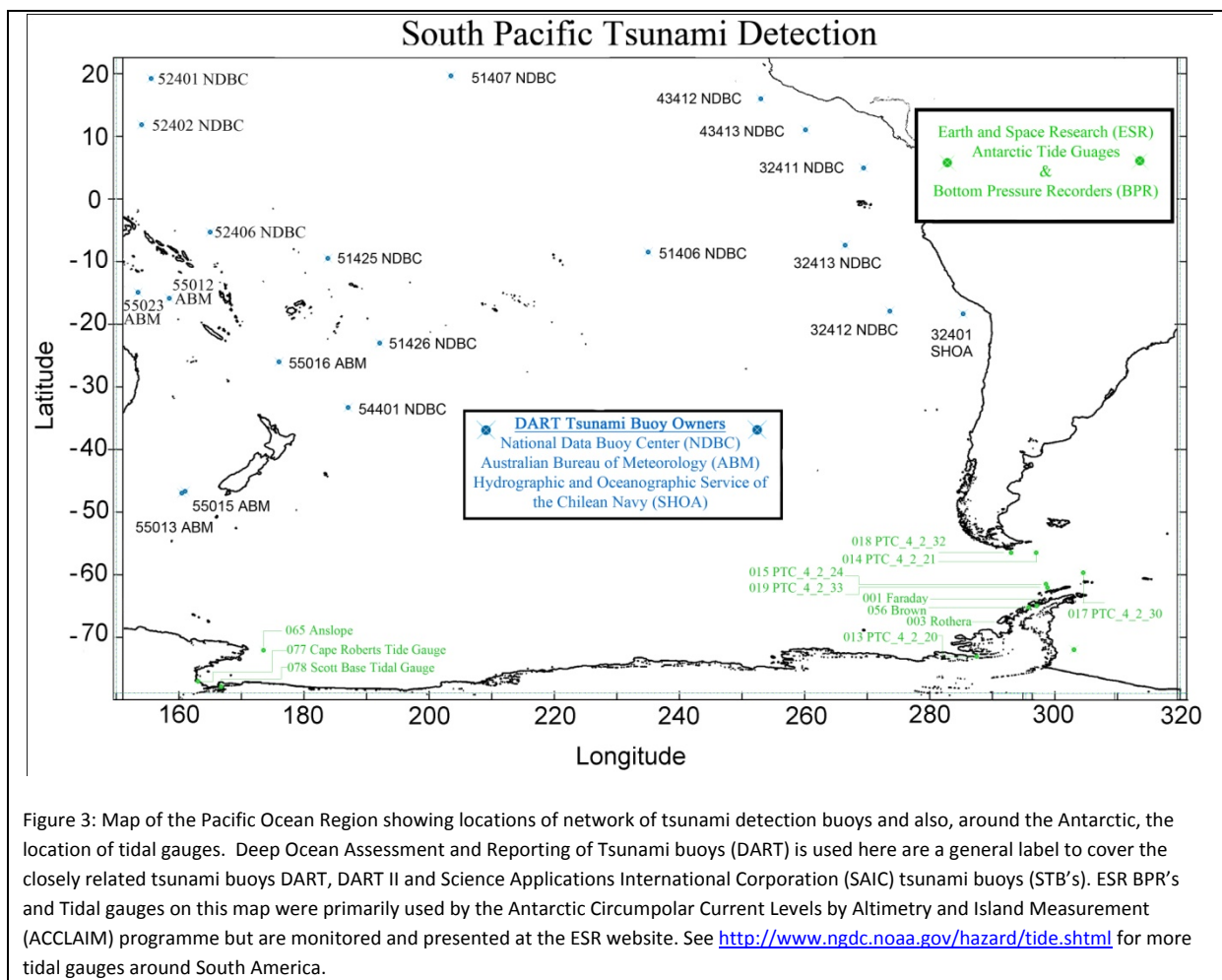


Figure 3: Map of the Pacific Ocean Region showing locations of network of tsunami detection buoys and also, around the Antarctic, the location of tidal gauges. Deep Ocean Assessment and Reporting of Tsunami buoys (DART) is used here as a general label to cover the closely related tsunami buoys DART, DART II and Science Applications International Corporation (SAIC) tsunami buoys (STB's). ESR BPR's and Tidal gauges on this map were primarily used by the Antarctic Circumpolar Current Levels by Altimetry and Island Measurement (ACCLAIM) programme but are monitored and presented at the ESR website. See <http://www.ngdc.noaa.gov/hazard/tide.shtml> for more tidal gauges around South America.

## Methodology

Before models can be run, geometric parameters about the specific plate boundary need to be known. These parameters are: fault length, fault width, epicentre, depth, strike, dip, rake or slip angle and dislocation (of the fault plane in meters). Parameters used in the models originate from journal articles from real earthquake events in the past, but in some cases, via interactive media from recognised organisations such as the United States Geological Survey (USGS) or earthquake data based used in the form of Google Earth KML files.

After obtaining the necessary parameters, a modelling area is defined and an equivalent and suitable bathymetry file prepared. The suitable file in this instance was downloaded at 4 arc minute resolution from the National Oceanic and Atmospheric Administration (NOAA) GEODAS Grid Translator.

Bathymetry is important, as it largely controls the wave-creating refractions, reflections, wave-guiding and dispersion effects. The reason the sea floor can produce these effects is because the tsunami propagates in the entire water column. Once the bathymetry is added, the COMCOT can then run at a matching resolution of 4 arc minutes grid size and at an appropriate 2.5 second time step resolution.

The COMCOT output files were then processed using Matlab. The images are available as Appendix 1 to this report and as a poster (which will be on view at the COMNAP AGM). The images and the known locations of Antarctic coastal infrastructure including research stations were then used to determine relative risk from tsunami to those station and occupying personnel. For this preliminary project, it was not possible to determine the effect that the presence of sea ice or ice shelves might have on tsunamis.

The images produced show maximum wave amplitude or equivalent sea surface elevation, obtained over the lifetime of the modelling. The maximum amplitude images (Appendix figures A1 – A11) have been processed up to three times each and the results have been combined using a simple image overlay technique. The result is a maximum amplitude image that contains three scales of tsunami wave height allowing more information to be displayed about the same event. Google Earth image overlay was further used as a common ground for analysis to view tsunami images in conjunction with tsunami buoy and base locations. In this report, the buoy locations have been superimposed onto some figures for convenience otherwise the reader can refer to Figure 3 to view the complete detection grid.

A series of these propagation images have been made into video files for further analysis.

## Modelling Considerations

COMCOT is capable of modelling the entire lifespan of a tsunami from initial water column displacement, through to the propagation of the tsunami across the ocean and also the inundation of selected areas. Hence, is very suitable for the modelling required. However, modelling in this report has not been done to the programmes highest potential as this would have been too timely, therefore reasonable approximations have been made. Further work could be undertaken in this manner if this initial project proves useful.

While linear shallow water equations have been used (figure 4), they cause the programme to under-evaluate tsunami wave height in regions where wavelength is large compared to the water depth (coastal regions and perhaps continental shelf). The physical effect neglected here, is coastal amplification or wave shoaling, and the rule of thumb is that the wave height can be approximately double of that of the open ocean (Brigadier *et al.* 1948 on wind derived waves). There are models that produce amplification factors that differ from those predicted by this rule, for example Satake (1992) observed an amplification factor of three. It should be noted that approximation of the amplification factor can be completely avoided if the non-linear equations are used.

Secondly, inundation modelling was not attempted due to the complexity it would have added. To model inundation, information regarding the Manning’s roughness coefficients for the Antarctic regions, i.e. rock, ice and building coefficients would have been needed. The coastal region of interest would then need to be mapped out and zoned by different coefficients before inundation is run. Due to Antarctica’s high seasonality, the coefficients would vary considerably throughout the year with the extent of the ice. These differences would mean that at least two Manning roughness maps would be needed to be produced. Using two maps would require each tsunami scenario to be run twice which is outside the time length of this project but could be undertaken in the next stage of this project. Modelling has been run at mean sea level, therefore, tides need to be considered when interpreting the results. Any risk analysis to the infrastructure should be done with high tide in mind, since it is at high tide that the structure will be the most vulnerable.

*The Linear Equations (Cartesian form):*

$\frac{\partial \eta}{\partial t} + \left\{ \frac{\partial P}{\partial x} + \frac{\partial Q}{\partial y} \right\} = -\frac{\partial h}{\partial t}$	$\frac{\partial P}{\partial t} + gh \frac{\partial \eta}{\partial x} - fQ = 0$	$\frac{\partial Q}{\partial t} + gh \frac{\partial \eta}{\partial y} + fP = 0$		
Equation 1.	Equation 2.	Equation 3.		
<p>where:</p> <table style="width: 100%; border: none;"> <tr> <td style="width: 50%;"> <p><math>\eta</math> is the water surface elevation.</p> <p><math>f</math> = Coriolis force</p> <p><math>x, y</math> and <math>t</math> are distance and time increments respectively</p> </td> <td style="width: 50%;"> <p><math>P</math> = volume flux (West – East)</p> <p><math>Q</math> = volume flux (South - North)</p> <p><math>h</math> = water depth</p> </td> </tr> </table>			<p><math>\eta</math> is the water surface elevation.</p> <p><math>f</math> = Coriolis force</p> <p><math>x, y</math> and <math>t</math> are distance and time increments respectively</p>	<p><math>P</math> = volume flux (West – East)</p> <p><math>Q</math> = volume flux (South - North)</p> <p><math>h</math> = water depth</p>
<p><math>\eta</math> is the water surface elevation.</p> <p><math>f</math> = Coriolis force</p> <p><math>x, y</math> and <math>t</math> are distance and time increments respectively</p>	<p><math>P</math> = volume flux (West – East)</p> <p><math>Q</math> = volume flux (South - North)</p> <p><math>h</math> = water depth</p>			

Figure 4: Equations used in the modelling software to produce the models.

Each model has been confined to an area, the boundaries of which behave differently depending on the type of boundary selected. The characteristics of the boundary selected can be reflective, absorbing or open. Two boundaries have been used in this report, the open boundary and the sponge boundary. The open boundary allows the tsunami to pass straight through it and the sponge boundary brings all physical properties to zero at the boundary. The sponge boundary is, physically, the more robust or physically reliable option, but it reduces the modelling area. It is the sponge boundary that is dominantly used in the models of this report.

COMCOT evaluates volumes fluxes and water surface elevations at the most basic level in square grids. It is in fact, an explicit, finite, “leap-frog”, difference scheme that evaluates this. Auto adjustment of the parent grid (the most basic layer) in COMCOT is an important choice for modelling at polar latitudes. Deformation of the grid squares occurs near the Polar Regions as squares of longitude and latitude in these regions are actually rectangular. Resizing of the COMCOT grid can be done to counteract this effect by selecting the Parent Grid’s ID Number to 0.

Essentially the models ran in this project show where the tsunamis from distant tectonic sources are directed to, in the vicinity of coastal Antarctica. What can be gained from the modelling is an approximation of tsunami arrival time, an approximation of tsunami wave height and an indication of the areas which are most or more often at risk or affected by a tsunami.

## Results

Ten models were run using information from earthquake events from the following:

Kermadec ABC (Full Fault Rupture)	Putsegur
Kermadec A	Aleutian 1946
Kermadec B	Chile 2010
Kermadec C	Chile 1960
Tonga 1865	Peru 1868

Table 1: The ten models that were run in the project.

The images produced after running the models can be found in Appendix 1 to this report. In all cases, the models showed that there would be some increase in maximum wave height, although in most cases that increase was relatively small (table 2).

Model	The Ross Sea	The Antarctic Peninsula
Kermadec ABC	0.075	0.075
Kermadec A	0.1	0.1
Kermadec B	0.1	0.1
Kermadec C	0.2	0.2
Tonga 1865	0.04	--not completed, ~ 0.1m as an estimate
Puysegur	< 0.05	no expected effects
Aleutian 1946	0.1 to 0.2 of tsunami wave entering the Ross Sea	0.5 to 1
Chile 2010	0.1	0.3
Chile 1960	0.4 to 0.45	0.6 to 1+
Peru 1868	0.5 in general, some areas up to 1.5.	From 0.5 (East) and greater than 1 (West) and up to 2 in some “pockets”

Table 2: Maximum expected wave heights in meters (without coastal amplification).

The results show, that there is a risk to coastal areas of the Ross Sea Region and to the Peninsula Region from tsunami, especially from tsunami which originate from and are on the order of the historical earthquake events of the Aleutian 1946, Chile 1960 and Peru 1868 (table 3). Since the research stations and various facilities and infrastructure are not at the same height (above mean sea level), a qualitative classification approach is used. The terms in the table have the meanings: Minimal = less than 0.1m; Slight = 0.1m to 0.3m; Moderate = 0.3m to 0.5m; Concerning = greater than 0.5m and can be greater than 1m.

<b>Model (see appendix)</b>	<b>The Ross Sea</b>	<b>The Antarctic Peninsula</b>
Kermadec ABC	Minimal	Minimal
Kermadec A	Slight	Slight
Kermadec B	Slight	Slight
Kermadec C	Slight	Slight
Tonga 1865	Minimal	Slight-Minimal
Puysegur	Minimal	Minimal if anything
Aleutian 1946	Slight	Concerning
Chile 2010	Minimal	Slight-Moderate
Chile 1960	Moderate	Concerning
Peru 1868	Moderate-Concerning	Concerning

Table 3: Qualitative risk, based on the tsunami models run for the Ross Sea Region and the Peninsula Regions.

A full discussion of the results can be found in Appendix 2.

## CONCLUSIONS

Of the ten models run for this project, the events of greatest concern to the Antarctic region are the 1960 Chilean tsunami, 1868 Peruvian tsunami and 1946 Aleutian tsunami. Models of lesser concern include Puysegur, Kermadec and Tonga. Hence the source or zone of greatest concern in regards to Antarctic coastal infrastructure appear to be from event originating from the Eastern Pacific Subduction Zones. Since the Chilean coast has produced many large tsunami events historically and it is quite close the Antarctic Peninsula this source is the greatest threat looked at in this report. But of course the models are based on very specific past events and conditions will vary.

The most vulnerable coastal Antarctic research stations in the Antarctic Peninsula region are Melchior, Actowski, Yelcho and San Martin as they sit at or below 5m. The Ross Sea Region's lowest research stations sit at 10m above sea level, so, are more protected from tsunami. However, large tsunami events could potentially affect this region. The bases in the Ross Sea are largely naturally sheltered from the brunt of tsunamis from the Pacific. Assessment of vulnerability is made via human extrapolation of the linear tsunami modelling in this report to account for the shoaling effects.

In terms of early detection, the tsunami buoys of greatest value, with respect to picking up large amplitudes of the tsunami models run are 32401 (off the coast of Chile/Peru) for the Peruvian



tsunami, 51406 (In the central Pacific) for the 1960 Chilean tsunami. All tsunami buoys can be directly monitored by Antarctic-based personal via the internet.

There are a host of other tsunami sources deserving attention of further modelling and research. Obtaining maps for the roughness coefficients of the research stations would be valuable so that inundation models could be run. Also the coefficients themselves may need to be reevaluated as no information was found on a value of propagation over (or under) an ice shelf.

This preliminary project has identified some key conclusions and comments for further consideration, listed here in no particular order:

- There is potential for some Antarctic research stations to be effected by tsunami under certain conditions mainly controlled by the tsunami source parameters and coastal amplification properties of coastal Antarctica. While the risk is general not high there is still a risk identified.
- The location for placement of any new DART buoys or other monitoring instruments must be carefully selected, as there are “good” and “bad” choices when it comes to early warning for the Antarctic coast. Tsunami buoy location may wish to intercept the most immediate threat or it may wish to be suitably deployed in a location which picks up the best range of large tsunami signals for a single coastline of interest (perhaps in areas of Antarctica where there are large numbers of people based). Alternatively a well placed tsunami buoy could be selected to benefit Antarctic programs and other countries of the South Pacific. If the last option on placement was the desired outcome it should be noted that this may have a slight trade off in effectiveness for the Antarctic regions considered here.
- The choice of monitoring device affects the quality of the data received, how often it is received and the cost associated with purchase, installation and maintenance.
- There seems to be a lack of a common qualitative ways of communicating tsunami risk and there is a need to identify an effective communications plan and system.
- The modelling program used in this report (COMCOT) had to be run on a setting such that the volume flux grid cells auto adjusted in the Polar Regions. It is important that any other tsunami modelling programs that attempt to model in the Polar Regions that they can in fact account for this. Also a suggestion to employ in further modelling would be to run the models at a higher resolution than 4 arc minute resolution, 1 and 2 minute data is available.
- Bathymetric data is required to improve modelling capability.
- No effects related to sea ice or ice shelf has been taken in to account when running this models.
- No effect related to boundary conditions at the Polar Convergence have been taken into account and all tsunami sources modelled are north of the Polar convergence and therefore would cross this boundary.
- Organisations with expertise in tsunami detection, modelling and research should work together with National Antarctic Programs on the next phase of this project.

## References

- Brigadier R. Bagnold A. Barber N, Deacon G and Williams W. 1948 Coastal Waves. Nature vol 192 pp 682-684.
- Fryer G. Watts P and Pratson L. 2004 Source of the great tsunami of 1 April 1946: a landslide in the upper Aleutian forearc. Marine Geology. Vol 203 pp. 201-218.
- Goff J. Walters R, Lamarche G, Wright I and Chaque-Goff C. Tsunami Overview Study 2005 Report for the Auckland regional council p4.
- Hayes G.P. and Fulong K.P. 2010 Quantifying potential tsunami hazard in the Puysegur subduction zone, south of New Zealand. Geophysics Journal International 183: pp1512-1524.
- Hidayat D. Barker J. And Satake K. 1995 Modeling the Seismic Sources and Tsunami Generation of the December 12, 1992 Flores Island, Indonesia, Earthquake. PAGEOPH 144: Kanamori H. and Cipar J. 1974 Focal Process of the Great Chilean Earthquake May 22, 1960. Physics of the Earth and Planetary Interiors 9: 128.
- Lopez A. and Okal E. 2006 A seismological reassessment of the source of the 1946 Aleutian 'tsunami' earthquake. Geophysics Journal International.
- Okal E. 2007 South Sandwich: The Forgotten Subduction Zone and Tsunami Hazard in the South Atlantic. *Eos Trans. AGU*, 89(53), Fall Meet. Suppl. Abstract OS51E-08.
- Okal E. Borrero J. and Synolakis C. 2004 The earthquake and tsunami of 1865 November 17: evidence for far-field tsunami hazard from Tonga. Geophysics Journal International 157: 168.
- Okal E. and Hartnady C. 2009 The South Sandwich Island Earthquake of 27 June 1929: Seismological Study and Inference on Tsunami Risk for the South Atlantic. South African Journal of Geology 112.
- Power W. and Gale N. 2011 Tsunami Forecasting and Monitoring in New Zealand. Pure and Applied Geophysics 168:1131.
- Satake K. 2005. Linear and Nonlinear Computations of the 1992 Nicaragua Earthquake Tsunami. PAGEOPH vol 144 nos 3/4 pgs 455 and 469 (whole paper is 455-470)
- Satake K. 2007. Tsunamis Elsevier 4:17,2.
- Satake K. and Kanamori H. 1990. Fault parameters and tsunami excitation of the May 23, 1989, MacQuarie Ridge Earthquake. Geophysical Research Letters. 7:997.
- Stirling M. McVerry G. and Berryman K. 2002 A New Seismic Hazard Model for New Zealand. Bulletin of the Seismological Society of America. 92: 1883, pp1898-1899.
- Tanioka Y. and Seno T. 2001 Detailed analysis of tsunami waveforms generated by the 1946 Aleutian tsunami earthquake. Natural Hazards and Earth System Sciences 1: pp171-175.
- Thomas C. Livermore R. and Pollitz F. 2003 Motions of the Scotia Sea plates Geophysics Journal International 155:785

Useful Websites:

Earth and Space Research (ESR)

[http://www.esr.org/antarctic\\_tg\\_index.html](http://www.esr.org/antarctic_tg_index.html)

Bottom Pressure Recorder (BPR) info (unofficial)

[http://www.oceans2025.org/PDFs/PDFs\\_of\\_powerpoints/Session\\_7B\\_Pete\\_Foden\\_POL.pdf](http://www.oceans2025.org/PDFs/PDFs_of_powerpoints/Session_7B_Pete_Foden_POL.pdf)

Global Disaster and Alert and Coordination System (GDACS)

<http://www.gdacs.org/>

Tropical Atmosphere Ocean (TAO) buoy dynamic height

[http://tao.noaa.gov/ftp/OCRD/tao/taoweb/deliv/cache/data4329/README\\_dyn.txt](http://tao.noaa.gov/ftp/OCRD/tao/taoweb/deliv/cache/data4329/README_dyn.txt)

National Data Buoy Center (NDBC)

<http://www.ndbc.noaa.gov/obs.shtml>

USGS rectangular earthquake grid search

[http://earthquake.usgs.gov/earthquakes/eqarchives/epic/epic\\_rect.php](http://earthquake.usgs.gov/earthquakes/eqarchives/epic/epic_rect.php)

New Zealand's tsunami gauges

<http://www.geonet.org.nz/tsunami/>

Antarctic Circumpolar Current Levels by Altimetry and Island Measurement (ACCLAIM)

<http://www.psmsl.org/links/programmes/acclaim.info.php>

<https://www.comnap.aq/facilities>

<http://www.ioc-sealevelmonitoring.org/map.php>

Intergovernmental Oceanographic Commission Tsunami Programme

International Tsunami Information Center. (ITIC)

<http://itic.ioc-unesco.org/>

United Nations Educational, Scientific and Cultural Organisation (UNESCO)

<http://www.unesco.org/>

**Acknowledgments**

Geological and Nuclear Sciences (GNS) Crown Research Institute, Wellington, New Zealand

Council of Managers of National Antarctic Programs (COMNAP)

University of Canterbury, Department of Geological Sciences

The University of Canterbury Summer Student Scholarship Scheme

## Appendix 1: Models

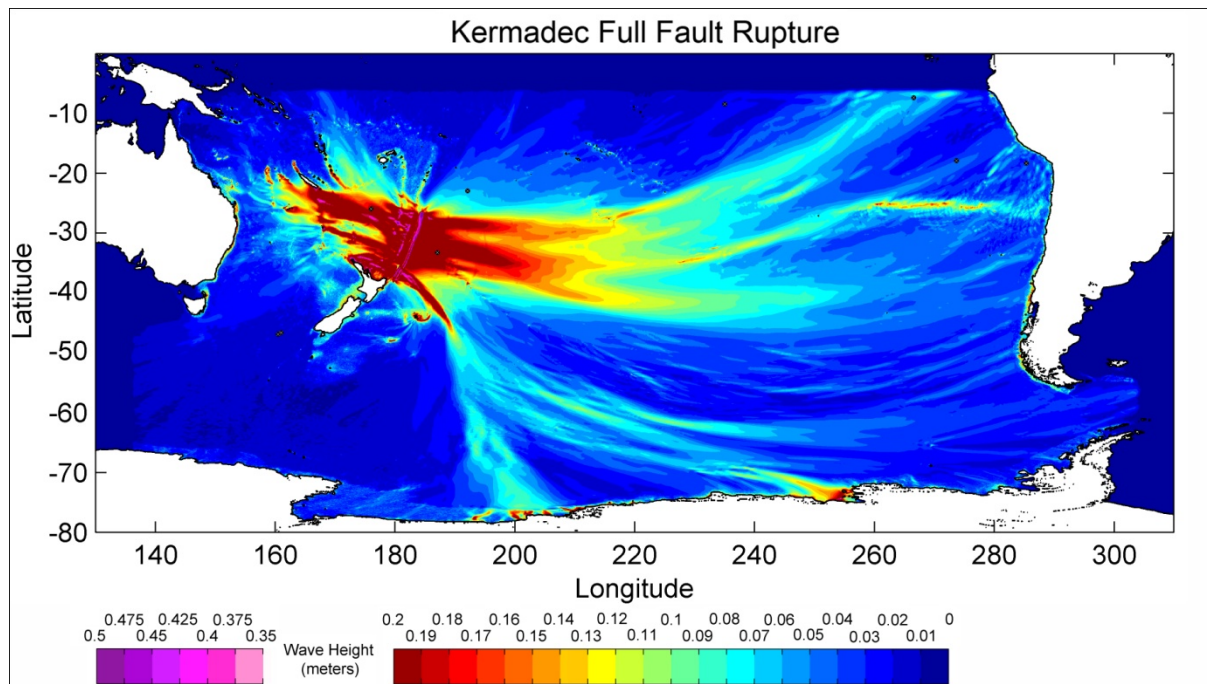


**Figure A1: Maximum Wave Amplitude of the tsunami from a rupture along the entire Kermadec subduction interface. Here the linear tsunami equations have been used.**

### Maximum wave height at DART tsunami buoy points:

55016 (0.2m), 54401(~0.2m), 51426 (~0.07m) and 32413 (0.07m)

### Arrival times and tsunami descriptions:

A line of latitude originating at Cape Adare heading south defines the Ross Sea arrival point from which the arrival time for all models is taken. For this model, the Ross Sea arrival time is 6 hours and 10 minutes. Here the tsunami is a very small negative amplitude wave that causes the sea to withdraw like a fast tide. The negative tsunami crest reaches the Antarctic Peninsula by 9 hours 30 minutes at Cape Byrd then Adelaide Island at 10 hours 10 minutes. A small positive tsunami crest follows the negative amplitude at the peninsula.

### Fault Mechanism Overview: *(supplied by GNS)*

Strike	Dip	Rake	Depth (range)	Dislocation	Length	Width	Number of Faults
191.7-212.4	4.0 - 17.5	90.0	3.97km-17.7km	2.2m	100km	50km	28

**Tsunami lifespan modelled: 15 hours.**

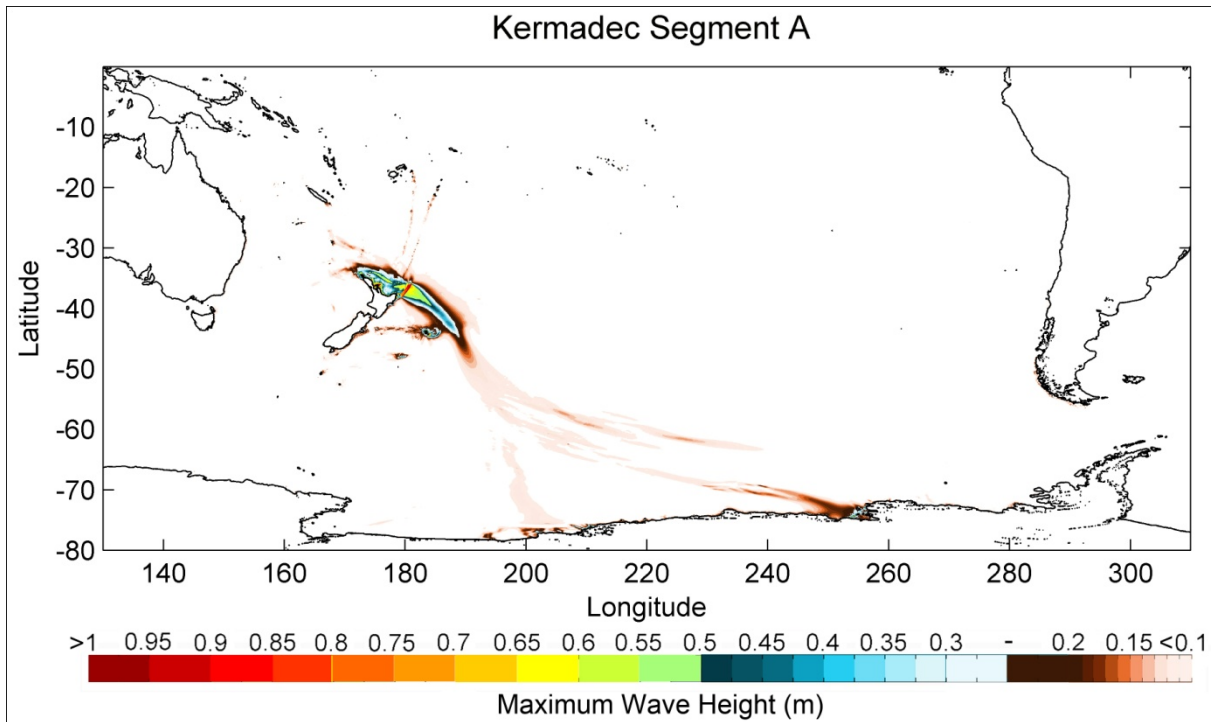


Figure A2: Maximum wave amplitude for a tsunami generated from the Kermadec A subduction segment

**Maximum wave height at DART tsunami buoy points:**

No tsunami waves are predicted by this model to be detected by any DART tsunami buoys.

**Arrival times and tsunami descriptions:**

Cape Adare arrival time: at 6 hours 10 minutes the first of a set of small tsunami waves arrive that later wrap into the Ross Sea Region. The largest tsunamis are 0.1m in size,

Cape Byrd arrival time: 9 hours 50minutes the arrival of tsunami not greater than 0.1m which is later followed by small tsunamis. The tsunami is directed at the Amundsen Sea and some of that energy is swept off toward the Antarctic Peninsula.

**Fault Mechanism Overview: (supplied by GNS)**

Strike (range)	Dip (range)	Rake	Depth	Dislocation	Length (segment)	Width (segment)	Number of Faults
202.9 – 212.4	4.0 – 11.4	90.0	3.97km- 10.36km	5.0	100km	50km	6

**Tsunami lifespan modelled: 15 hours.**

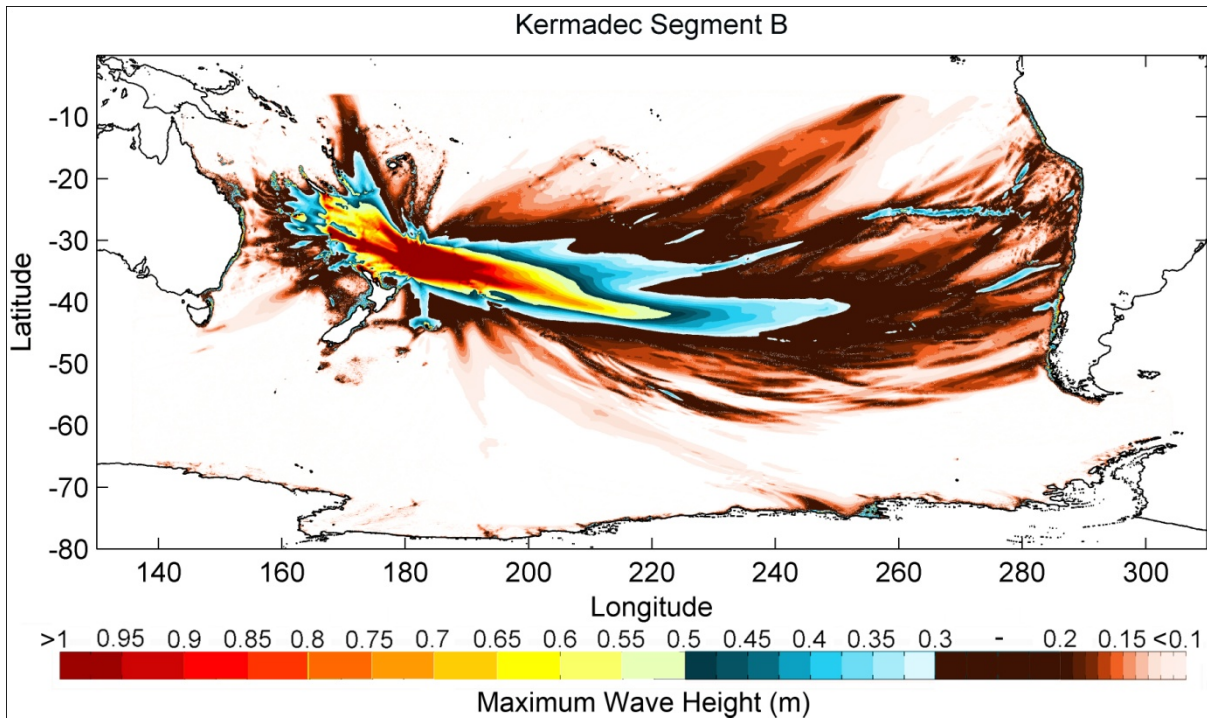


Figure A3: Maximum wave amplitude for a tsunami originating from a Kermadec B segment slip.

**Maximum wave height at DART tsunami buoy points:**

- 54401 (greater than 1m),
- 55016 (0.5-0.3m);
- 51426 (0.15m)

**Arrival times and tsunami descriptions:**

Ross Sea arrival time: 6 hour 10 at Cape Adare (0.1m wave)  
 Peninsula arrival time: Cape Byrd: 9 hours 40 minutes, Adelaide Is.: 10 hours 20 minutes  
 and at South Shetland Is: 10 hours 30 minutes. All tsunami waves are small and of about 0.1 meters in height.

**Fault Mechanism Overview** (supplied by GNS)

Strike (range)	Dip (range)	Rake	Depth (range)	Dislocation	Length (segment)	Width (segment)	Number of Faults
196.9 – 205	5.8 – 15.4	90.0	5.0 – 15.1km	10.0m	100.0km	50.0km	11

**Tsunami lifespan modelled:** 19 hours.



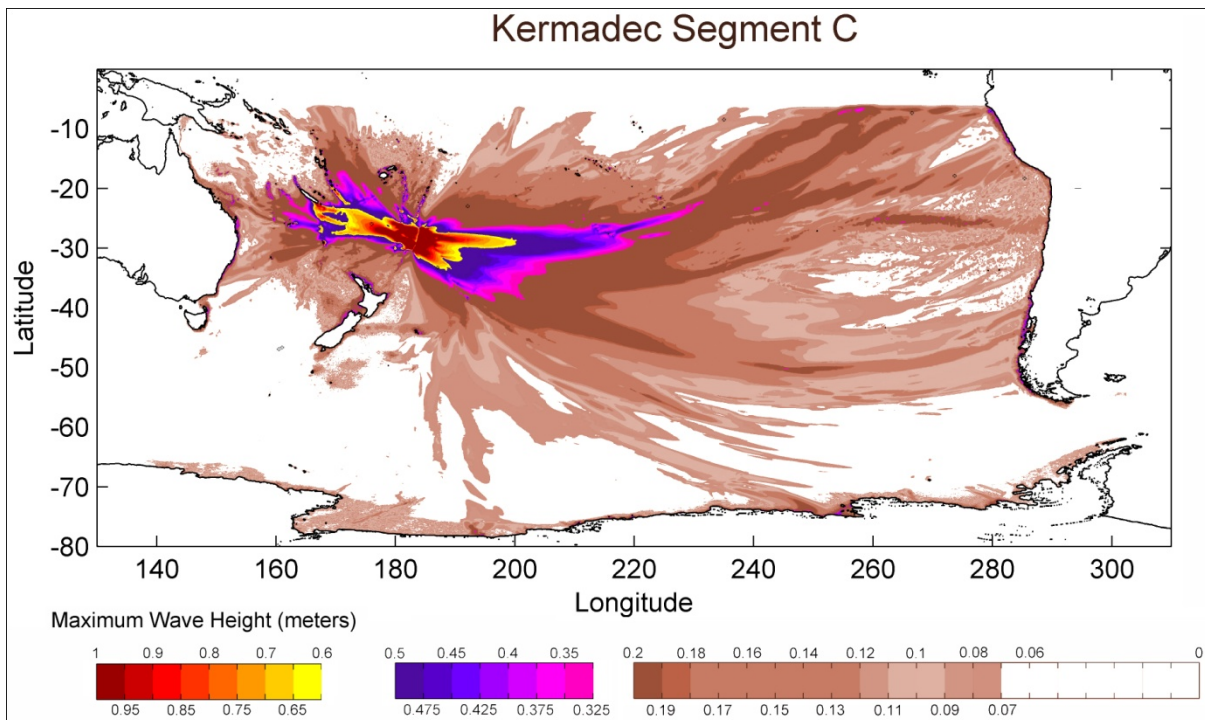


Figure A4: Maximum wave amplitude for a tsunami generated from a slip on C segment of the Kermadec trench.

**Maximum wave height at DART tsunami buoy points:**

55016 (0.9 to 0.85m), 54401 (0.65 to 0.6m) and to a lesser extent 51426(0.2m), 32413(0.18 to 0.12m), 32412 (0.18 to 0.12m) and 32401(0.09 to 0.07m).

**Arrival Times and Tsunami Descriptions:**

Ross Sea arrival time: 6 hours the draw-back arrives followed by a small 10cm tsunami half an hour later.

Antarctic Peninsula receives the drawback at 10 hours and 10 minutes followed by a 10cm tsunami at 11 hours at Cape Byrd.

**Fault Mechanism Overview (Supplied by GNS)**

Strike (range)	Dip (range)	Rake	Depth (range)	Dislocation	Length (segment)	Width (segment)	Number of Faults
191.7 – 202.8	9.55 – 17.47	90.0	6.51 – 20.0km	8.0km	100km	50km	10

**Tsunami lifespan modelled: 20 hours.**

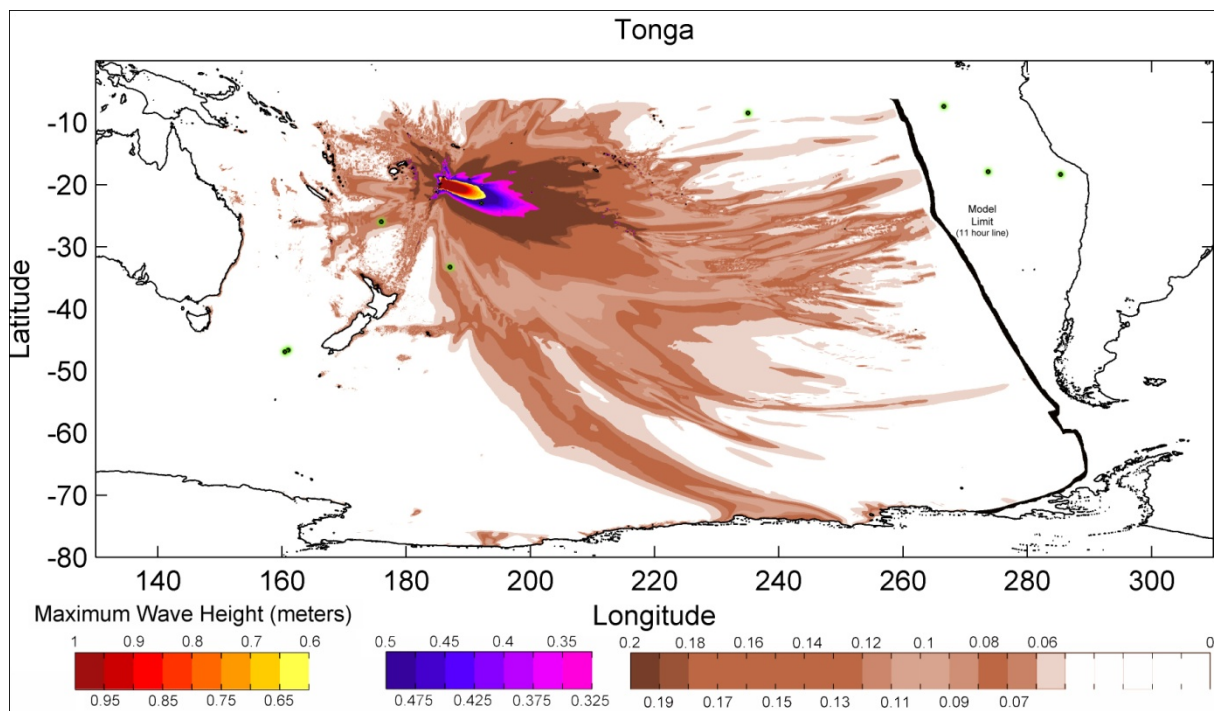


Figure A5: Maximum wave amplitude for the tsunami in 1865 originating offshore of Tonga.

**Maximum wave height at DART tsunami buoy points:**

51426 (0.5 m), 54401(0.1m) and 55016 (0.08m)

**Arrival Times and Tsunami Descriptions:**

Antarctic Peninsula arrival time: 10 hours 30 minutes (maximum between 11 and 12 hours)

Ross Sea arrival time: 6 hours 30 minutes the tidal retreat occurs, followed by a 10cm tsunami at 7 hours and 40minutes and the maximum water height in the bay occurs between 8 and 9 hours)

**Fault Mechanism Overview: (Model 1 in Okal *et al.* 2004)**

Strike	Dip	Rake	Depth	Dislocation	Length	Width	Number of Faults
198.0	45.0	90.0	25.0 km	5.2 m	177.0 km	88.0 km	1

**Tsunami lifespan modelled: 11 hours.**



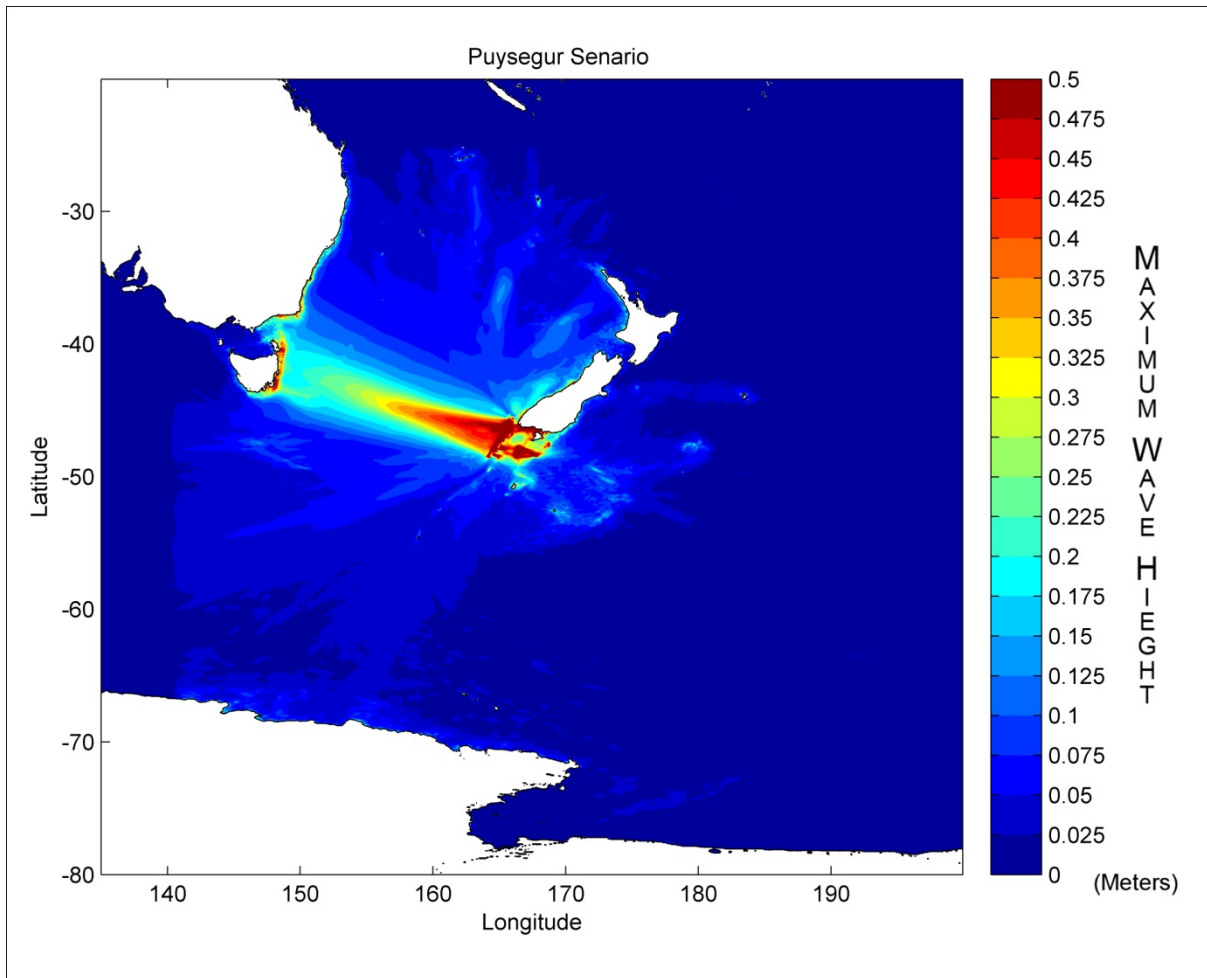


Figure A6: Maximum wave amplitude for a tsunami originating from an oblique slip on the Puysegur subduction zone

**Maximum wave height at DART tsunami buoy points:**

55015 (0.2m) and 55013 (0.35m)

**Arrival times and tsunami descriptions:**

The tsunami reaches Cape Adare at 3 hours and 20 minutes with an amplitude of 1cm. The largest waves travelling into the Ross Sea during the 10 hours modelled do not exceed 5cm. Antarctic Peninsula is not likely to receive any significant tsunami as the wave crest height heading East is a mere 2.5cm.

**Fault mechanism overview: (Hayes and Fulong 2010)**

Strike	Dip	Rake	Depth (range)	Dislocation	Length (range)	Width (range)	Number of Faults
19.0	13.5	144.0	4.0 – 27.9 km	4.0m	134.6 – 318.1 km	17.68 – 32.28km	5

**Tsunami lifespan modelled: 10 hours.**

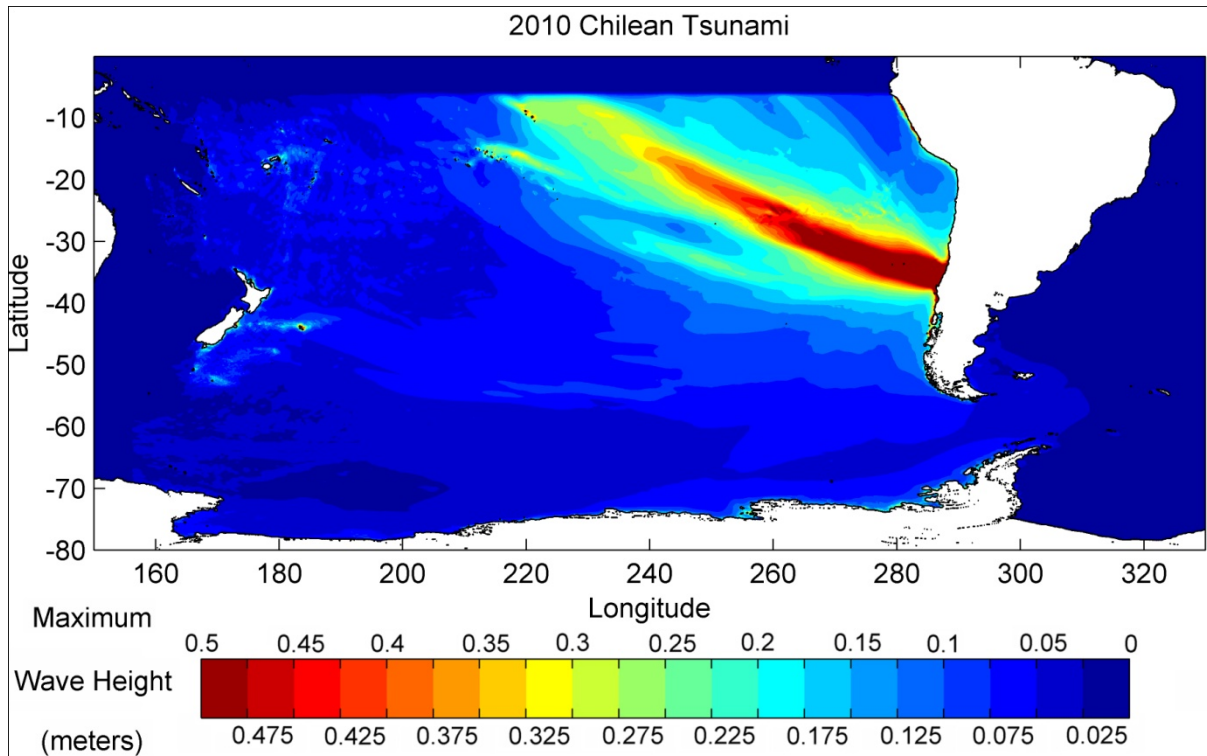


Figure A7: Maximum wave amplitude of tsunami from the 2010 Chilean subduction interface slip.

**Maximum wave height at DART tsunami buoy points:**

32412 (0.2m)

**Arrival times and tsunami descriptions:**

Tidal drawback starts at the peninsula is at 1 hour for the South Shetland Islands and 50 minutes later at Adelaide Island and 2 hours 20minutes at 1. At 4hour 40minutes a tsunami arrives at the Shetland Is rising to a maximum at 5-5.5 hours of 0.3m. The tsunami reaches Adelaide Is. and Cape Byrd at 5 hour 30minutes. It enters the Ross Sea at 9 hours and 40 minutes after the initial fault rupture and is smaller than 10cm.

**Fault Mechanism Overview: (GNS model)**

Strike	Dip	Rake	Depth	Dislocation	Length	Width	Number of Faults
16.0	14.0	104.0	35.0 km	9.5m	420.0 km	100.0km	1

**Tsunami lifespan modelled: 20 hours.**

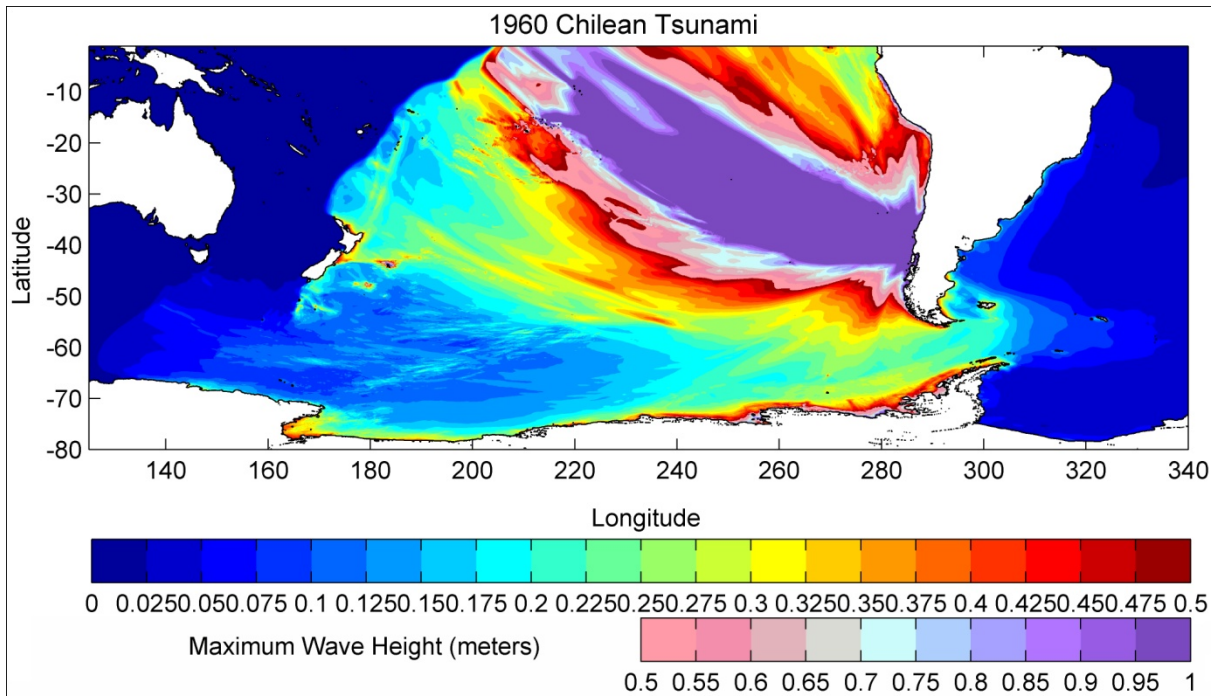


Figure A8: Maximum wave amplitude for the 1960 Chilean tsunami.

**Maximum wave height at DART tsunami buoy points:**

51406 (1m >) to 32413(0.375 to 0.35m), 32412(0.375 to 0.35m), 32401 (0.5m), 51426(0.175 to 0.15m), 55016(0.175 to 0.15m) and 54401(0.225 to 0.2m)

**Arrival Times and Tsunami Descriptions:** Arrival times have at least a +/- 5 minute uncertainty.

At 3hours and 50minutes\* the first tsunami wave reaches the South Shetland Islands. The tsunami wraps around Adelaide Island and into Marguerite Bay at 4 hours 30minutes.

Maximum water height in the bay occurs between 5 hours 40 minutes and 6 hours 20 minutes and ranges from 60cm up to 1m before considering shoaling effects. Nine hours after rupture the tsunami reaches the Ross Sea, but the maximum amplitude arriving between 11 and 12 hours of approximately 0.4 meters. The first wave reaches Adelaide Island at 21 hours which is promptly followed by two larger (0.5 meter) tsunami within the hour. No description is given for the South Shetland Islands as they are within the sponge boundary for this model.

**Fault mechanism overview:** (Kanamori and Cipar 1974)

Strike	Dip	Rake	Depth	Dislocation	Length	Width	Number of Faults
10.0	10.0	80.0	30.0km	24.0m	800km	200.0km	1

**Tsunami lifespan modelled:** 13 hours.

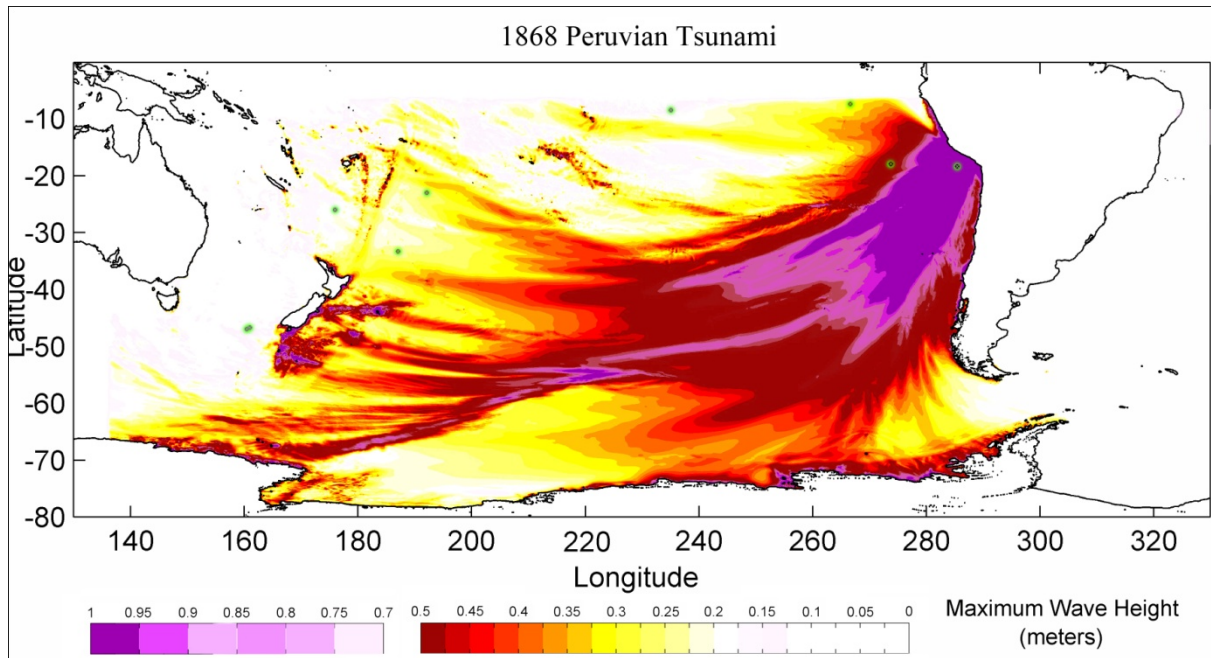


Figure A9: Maximum wave amplitude for the 1868 Peruvian tsunami.

**Maximum wave height at DART tsunami buoy points:**

32401 (2m +), 32412(0.55 to 0.6m) and 32413 (0.3 to 0.25m)

**Arrival times and tsunami descriptions:**

Antarctic Peninsula first arrival time: 7 hours 30minutes the tsunami hits the South Shetland Islands. Ross Sea first arrival time: 12 hours 30minutes the first of a set of 25cm waves arrives. See the nested grids (Figures 13 and 14 for further detail on the largest waves)

**Fault Mechanism Overview:**

Strike (range of)	Dip	Rake	Depth	Dislocation	Length (range)	Width	Number of Faults
305 to 316	20.0	90.0	20.0 km	15.0m	600km to 300km	150km	2

**Tsunami lifespan modelled:** 20 hours.

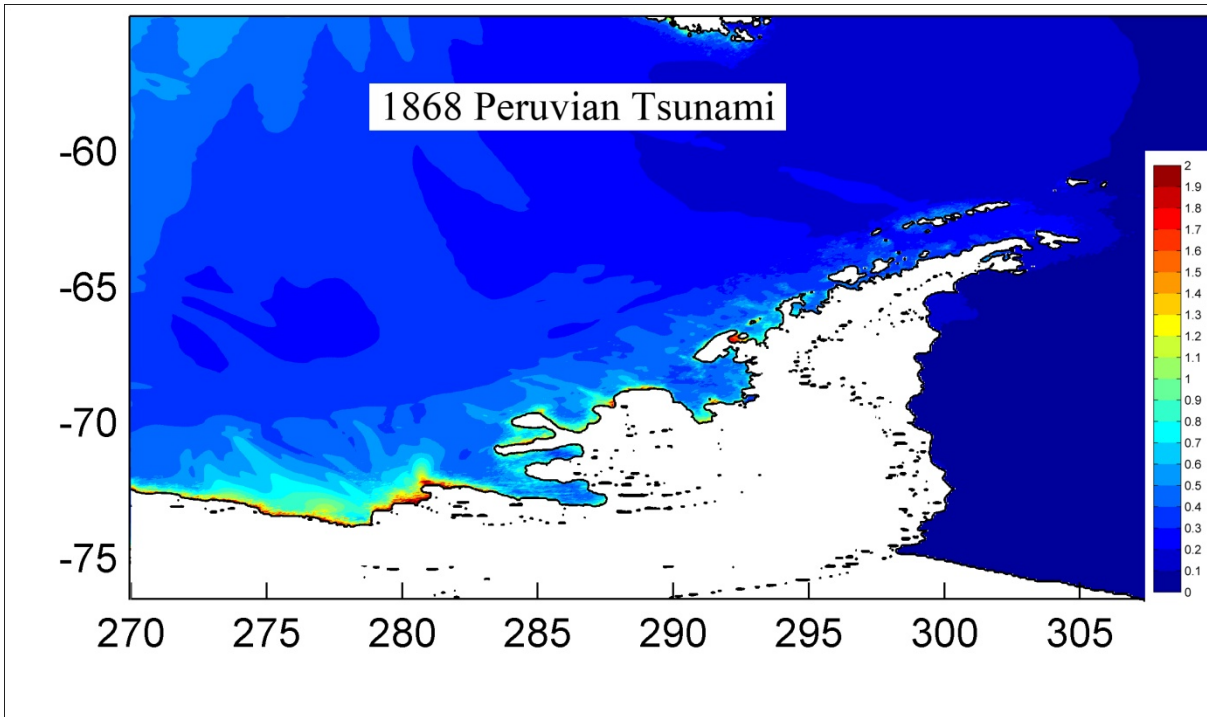


Figure A10: A nested grid (still at 4 arc minute resolution) showing the maximum wave amplitude at the Antarctic Peninsula for the 1868 Peruvian tsunami.

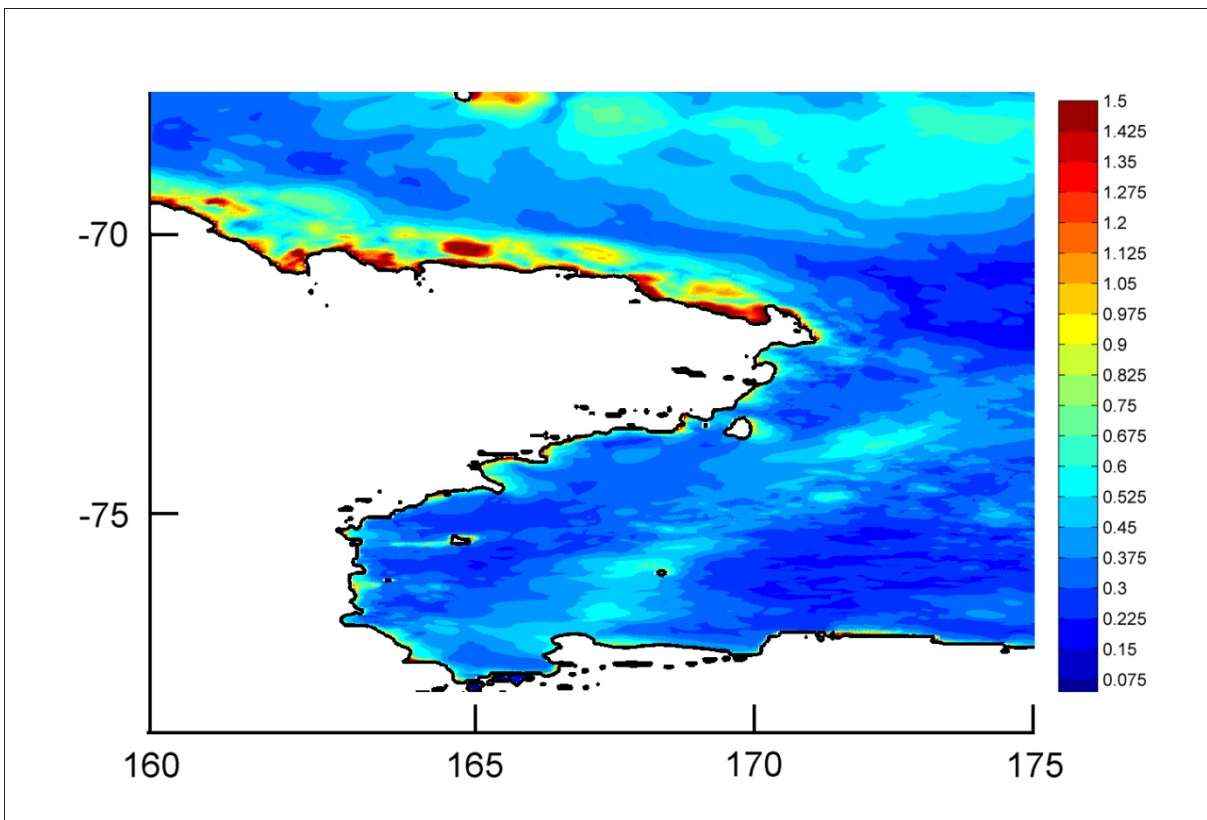


Figure A11: The nested grid (at the same resolution) showing the maximum wave amplitude at the Ross Sea region for the 1868 Peruvian tsunami.



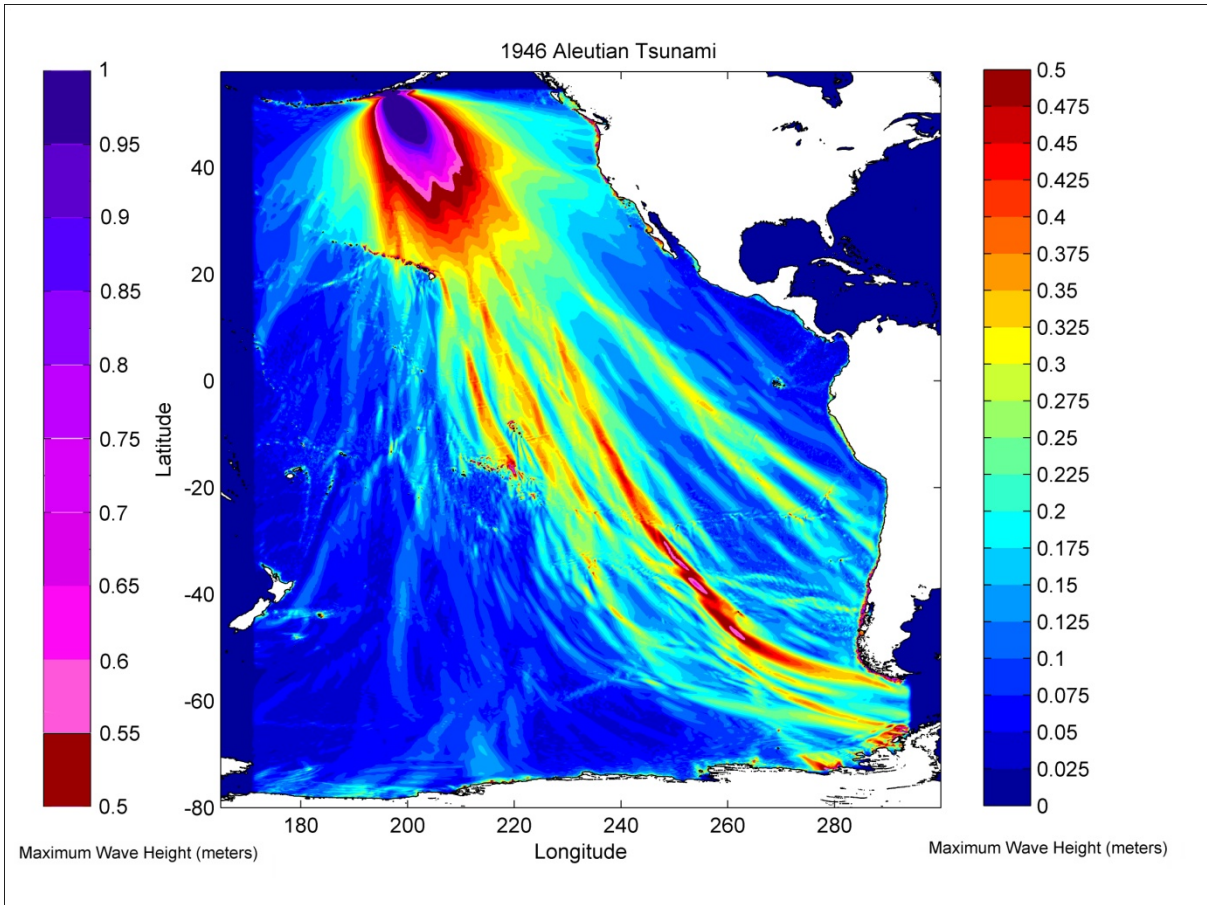


Figure A12: The Maximum wave amplitude for the 1946 Aleutian tsunami with uplift of sediments incorporated into the modelling parameters.

**Maximum wave height at DART tsunami buoy points:**

46408 (1m+) and 46403(0.5m) are buoys near the source offshore of the Aleutian trench (two of many northern Pacific buoys that best measure this tsunami), 51406 (~0.5m), 32412 (~0.3m) and 51407(0.2m) which is just south of Hawaii.

**Arrival times and tsunami descriptions:**

This model produces a much larger secondary tsunami wave than the first tsunami wave. The Ross Sea receives a tsunami not greater than 5 cm at 18 hours and 30 minutes. The Antarctic Peninsula receives a 0.5m tsunami everywhere and in parts up to 1m. Arrival times of the first wave are at 20hours 50 minutes at Adelaide Is. and 21 hours at Cape Byrd. South Shetland Islands are affected by the sponge boundary and no reading can be given here.

**Fault Mechanism Overview: (Tanioka Y. and Seno T. 2001)**

Strike	Dip	Rake	Depth	Dislocation	Length	Width	Number of Faults
250.0	6.0	90.0	30.0km	27.5m	160.0km	30.0km	1

Tsunami lifespan modelled: **23 hours.**

## Appendix 2: Full Discussion of Results

### The Models

Models of historic tsunami or probable tsunami generating scenarios have been selected from various sources to try and give a good coverage of the different directions that a tsunami might realistically approach the Ross Sea or Antarctic Peninsula (the regions are affected differently depending on the model).

### **Chilean Tsunami Models** (See Figures A7 and A8)

Two of the tsunamis were modelled from the Chilean Subduction source were from large energy tectonic ruptures; they were generated by the 9.5 magnitude earthquake in 1960 and the 8.8 magnitude earthquake of Concepcion in 2010. The 1960's tsunami is of great historical significance as it affected a large portion of the Pacific as well as being devastating locally. The Concepcion tsunami is a more recent event, smaller in size but relatively similar in location. Notably there has been other large tsunamis in history originating from the South America subduction system and therefore more far-a-field tsunamis are reality from this source in the future.

The 1960 model shows an effect in the Antarctic regions, forecasting for the Antarctic Peninsula a maximum (linear) wave between 0.6 and 1m for most of the region with some localities receiving waves in excess of 1m. For the tsunami the Ross Sea is expected to receive about half a meter before amplification. The model of the 2010 tsunami shows that the Antarctic region may only just be able to detect the tsunami and the Ross Sea may not even be able to do that. The comparison between the 1960 and 2010 models illustrate a massive variability of threat arising from sea floor deformations occurring on the Andes subduction zone. Thus the exposure of Antarctic personnel to a dangerous tsunami from the Chilean area needs to have the input of active monitoring so that a threat to the Antarctic region from the Chilean Subduction interface can be distinguished. Greater coverage of tsunami buoys in the low latitudes in the Pacific Ocean would be helpful so that this could occur. If more buoys were present, then more reliable warnings could be given and appropriate responses initiated.

### **The 1946 Aleutian Tsunami** - See Figure A12

The Aleutian tsunami was generated by an 8.1 magnitude earthquake, a relatively small magnitude quake considering the tsunami large height that resulted. Local to the source at Unimak Island, run-up is thought to have reached a colossal 42m (Lopez and Okal 2006) or 35m (USGS database) which is still very large. Theories as to why this happened include submarine landslide models and uplift of sediments. This modelling in this report incorporates the additional uplift of sediments which has been taken into account by increasing the fault displacement (Tanioka and Seno 2001). Historically there have been other significant tsunamis from the Aleutian Subduction zone of the Northern Pacific namely, to the East the 1964 Alaskan tsunami and further west the 1957 Aleutian and 1952 Kamchatka tsunamis. Having one model run from this region provides a more global understanding of the possible tsunami threats posed to the Antarctic region. When a tsunami next occurs from a Northern Pacific subduction zone it will be well covered initially by Northern Pacific tsunami buoys. By the time the tsunami enters the Southern Pacific the tsunami's characteristics will be better understood. In the Aleutian scenario modelled here the Antarctic Peninsula is expecting waves of around 1m (before shoaling) while the Ross Sea region does not receive any tsunami waves. The reason for this is the tsunami was highly confined in wave front width as travelled toward the South (evident in [Figure 15.](#)) Supporting evidence for a large tsunami from this model is provided by historic tsunami run-up records (Fryer *et al.* 2004). Fryer *et al.* show that the peninsula received run-up heights in the range of 1 to 4 meters.

Limiting the modelling of the Aleutian tsunami is the sponge boundary found to have an effect in the more eastern region of the peninsula. The result of the boundary is what looks like tsunami waves between 10 and 20 cm in size. This edge region is misleading as modelling here is subject to damping of actual wave heights expected. The location of the boundary could not be changed because of the restrictions placed on the largest bathymetry file able to be downloaded. Such a boundary was required for the large travel times associated with the scenario to reduce other unnatural effects. Large modelling times are a follow on of large travel times and unfortunately modelling was cut short due to the model not being pre-programmed to run long enough. The shortcoming results in the largest tsunami wave stopping just short of the coast in the lowest latitudes. Even so, the model has proven that the waves from this source stops can be expected at the Antarctic Peninsula although the



full effects are unknown.

### **The (1868) Peruvian Tsunami** See Figure A9

The Peruvian tsunami is generated from an 8.5 magnitude earthquake having a dislocation of 62.5% and a rupture area of 28.6% of that of the 1960 Chilean Tsunami. Yet the Peruvian tsunami produces the largest tsunamis modelled here in this report for coastal Antarctica. The reason is because the Peruvian segment is orientated such that tsunami originating from it are directed at coastal Antarctic. That is, the source is efficient at preserving wave heights in Antarctica's direction.

This model has additional information in the form of nested grids (see Figures 13 and 14) to provide added detail to the coastal regions of interest. Figure 14 reveals within the Ross Sea region on the coast near the Mario Zuchelli base a larger tsunami height of 1.5 meters is expected (three times larger than any other tsunami waves in the region). The Mario Zuchelli, sits at 15m and therefore an impossible high amplification factor of 10 would be needed for the station to be hit directly with a wave. Run up however is a slightly different to maximum expected wave height as it depends on the volume and velocity of the driving waters behind it. The Antarctic Peninsula can expect waves of larger than 1m (without coastal amplification)

### **Kermadec Trench Tsunami Models** - See Figures A1, A2, A3 and A4

Modelling along of tsunami from the Kermadec subduction zone consisted of four different rupture scenarios. All scenarios appear not to affect the Antarctic regions in any significant way. No models produce waves with maximum wave heights greater than 20cm. Threat from such a tsunami would likely only be from surging seaways perhaps unsuitable for small water craft in coastal areas. The region that most consistently receives the larger tsunami waves from this source is the unpopulated Amundsen Sea. This may need to be considered for any potential projects planned for the future in the area. One of the models, Kermadec Segment A produces a small far field tsunami; however, the 5m fault displacement parameter used is also relatively small. If a larger displacement were to occur the direction that this wave travels could have greater implications for the Antarctic Peninsula but not likely to the extent that the South American events would.

Kermadec segment B, produces the greatest tsunami for the whole of the Antarctic coastline compared to the other Kermadec models. It is also this segment that has the largest predicted fault displacement and here in lies the cause.

### **Puysegur Scenario** See Figure A6

The energy from a rupture on the Puysegur subduction interface results in water surface displacement that sends highly directional waves toward Australia and away from any areas of interest of this study. Waves produced by this scenario are relatively small like the fault displacement which the model is run from. If a larger displacement than four meters were to occur then perhaps a small tsunami would be detected at the Ross Sea region. Tsunami buoys 55015 and 55013 are a proven necessity to provide warning for Australian coastal regions and cities such as Hobart

Historically in the USGS database the 1989 quake having a depth of 10km and being of large magnitude (8.3) would suggest that this southern extension of the Puysegur trench could be a candidate for further tsunami modelling. The largest expected waves are very small and not likely to exceed 5cm if they even made it the distance to the Ross Sea or Antarctic Peninsula.

### **Tonga** - See Figure A5

The Tongan model produces small tsunami waves for the peninsula and Ross Sea regions. In comparison to the other smaller tsunamis of the West Pacific: Kermadec Segment A has a similar displacement and produces a far smaller tsunami. The reason for the smaller tsunami is because of the orientation of the fault rupture plain.

This model is stopped at 11 hours which is before the tsunami arrives at the peninsula. Figure A5 and video analysis tend to suggest that any tsunami reaching the peninsula will be small. The largest expected waves (without coastal amplification are)

### Other Potential Tsunami Sources

The Scotia / South Sandwich plate boundary is an active subduction zone near the Antarctic Peninsula that was not modelled in this report. Information on tsunamis generated from the

region was not found but the region shows a reasonable seismicity using the USGS's Google earth files and it is an active plate system. One paper breaks down the plate boundary into six segments using a statistical binning approach. In each of the geographical bins earthquakes shallower than 60km and placed, then averaged to produce segments contains the averaged parameters for strike dip and rake in the form of a double couple solution (Thomas *et al.* 2003). Other data in there paper could be reworked to produce some of the other parameters needed (e.g. average depth) for tsunami modelling which could be used in conjunction with reasonable assumptions on the dislocation to produce some tsunami models from the South Sandwich subduction zone. Okal and Hartnady 2009 ran a model using the program Method Of Splitting Tsunamis (MOST) from a magnitude 8.3 earthquake centred on the northwest corner of the Scotia arc. The model was based on the earthquake in 1929 and the model predicts 10 to 20cm waves (before coastal amplification) for the East coast of the Antarctic Peninsula.

A model could not be run from the southern extension of the Kermadec subduction zone, Hikurangi trench because of the uncertainty in the dislocation parameter. It is not really known how much dislocation occurs on the fault plane when it ruptures (Stirling *et al.* 2002). An additional tsunami hazard in the form of submarine landslide is also a point of concern for the Hikurangi trench system (Goff *et al.* 2005). Earthquakes on the trench may generate a tsunami from the faulting and trigger a submarine landslide the result of which being additive.

The San Andreas Fault lies on the Pacific rim but was not looked at due to time constraints but could be a possible source to model. A historic tsunami in 1992 generated by the strike slip system produced significant local tsunami at Cape Mendocino but it is not expected to have far-field consequences (González *et al.* NOAA Website)

There are a host of fault sources around the Antarctic region which may be able to generate a local tsunami. A good example is the Macquarie Ridge earthquake 1989 for there is a record of small tsunami waves landing in Australia (Satake and Kanamori 1990). Using the USGS's rectangular area tool a there are a series of magnitude 6 earthquakes on the South Pacific. Any large rupture generating offshore of southern Chile would have a very short travel time to the Antarctic Peninsula adding a level of danger as the chances of catching people unaware

is much higher. Earthquakes of less than  $M$  6.5 generally do not produce surface ruptures (e.g., Wesnousky, 1986)

#### Comments and Other Considerations

The frequency of tsunami source events has not been considered in this report but is an important factor that needs to be incorporated when considering the risk that a particular scenario poses. Tsunamis generated less frequently should be given a lower risk weighting than the same sized tsunami produced more frequently from a different source. The frequency of event may influence the placement location of any tsunami buoys deployed in the future. Location of tsunami buoys is a key issue, as poor, perhaps unlucky, placement can yield a tsunami threat being down-played as the worst of the tsunami does not pass through the buoy point.

Research stations may be above any expected tsunami level but that does not mean that the whole of their operation is at or above the reported altitude. Many bases that are close to the coast likely have boating access to the water hence at certain times personnel may be below a safe height or be on the water and critical marine infrastructure may also be at risk. Exposing themselves like this may be daily routine and so providing adequate warnings to the Antarctic coastal regions could save lives.

If possible it would be useful to compare the actual tsunami size with what the model height is at known locations to see what kind of amplification factor we might expect.

When viewing the maximum amplitude files in detail there is a need to consider the limitations of the modelling created from using the linear equations: coastal amplification, wave path, wave breaking, and other effects. As the tsunami's wavelength becomes comparable to the water depth the bottom friction becomes important. The effect of using the non linear equations to the wave motion is to give more control to the sea floor. Tsunami will diffract into bays to a much greater extent due to the added friction. The bases of the Antarctic Peninsula that are on sheltered side of an island or bay will experience more of an effect. There is also the coastal amplification of the wave height and an expected delay in the arrival times given.

All fault ruptures have been assumed to be instantaneous when in reality ruptures do have a

propagation time. Thus some variation can be expected from the models presented in here from this assumption.

Antarctica generally has a large time frame before a tsunami reaches it. The shortest (linear) travel time of any tsunami modelled (regardless of its size) to the Peninsula is from the 1960 Chilean tsunami source having a travel time of around 3hours. Closer tsunami sources do exist for the Antarctic Peninsula; the southern extension of the South America trench, the plate boundaries associated with the Drake Passage as well as local submarine landslide and volcanic sources.

#### Added dangers associated with tsunami in Polar Regions

Tsunamis in this report are perhaps not threatening to the majority of Antarctic facilities but, tsunamis in Polar Regions are far more dangerous to the individual than in warmer climates. A small tsunami may be strong or high enough to topple a person over. If a person is swept of their feet in polar waters the consequences is far more life threatening than in the tropics. Surges can drag people out to sea and often the Antarctic sea regions are edged with rock and ice cliffs. Any damages occurring to Antarctic buildings or sea craft has greater implications as repair or replacement is more limited in these distant and extreme environments, especially for those coastal Antarctic stations that support winter-over personnel. Winter brings with it an added vulnerability to people because of the darkness and the lower temperatures. Less people will be exposed to tsunami threat in the winter as many coastal research stations only operate in the summer season.

#### Environmental Concern: Ice Shelf Instability

The ice shelves and winter sea ice may be a useful tsunami buffer and damping mechanism. A tsunami propagating under an ice shelf may cause the ice shelf to fracture under the pressure of the positive crest. Furthermore the negative crest creates an air gap leading potentially to sagging of the ice layer or if the change is rapid a suction effect may be possible on the ice body. These added forces may damage or weaken the ice shelf and the effects should be investigated further.

#### Tsunami Detection

For a tsunami warning system to be effective, a tsunami must first be detected and then the information must be communicated quickly to all potentially affected regions. Seismic waves

from earthquakes centred in submarine settings give early warnings to scientists that a tsunami may have been generated. Coastal regions local to the source may not get any official warning before a tsunami reaches them, as it depends on whether a warning system is in place and how far away the tsunami is. Distant coastal populations away from a tsunami source should receive warning of a potential tsunami threat, as there is time to evaluate the tsunami's propagation if it is checked by suitable buoys. Another option to obtain information on the tsunami's likely path is by modelling (requires parameters of the generation mechanism which have to be assumed or have become available through seismic analysis). Parameters (fault, width and length) used in the tsunami modelling can be estimated using the accumulation of aftershocks on the fault plane. Aftershocks, however, reveal the fault plane over a period of time, making real time modelling by this method problematic. Quick warnings may also be achieved once the magnitude of the earthquake is known by reviewing pre-event constructed models; as practiced by Global Disaster Alert and Coordination System GDACS.

### Appendix 3: Predicted Maximum Wave Heights at Buoys

Buoy	55016	54401	51426	32413	32412	32401	55015	55013	51406	46402	46403	51407
<a href="#">Figure 4.K</a>	0.35- <b>0.20</b>	0.20- 0.21	0.07- 0.06	0.07- 0.06	0.05- 0.04	0.05- 0.04	0.02- 0.01	0.02- 0.01	0.03- 0.02	<i>b</i>	<i>b</i>	<i>b</i>
<a href="#">Figure 5.KA</a>	0.03- 0.04	0.07- 0.08	0.03- 0.04	0.01- 0.02	0.02- 0.03	0.01- 0.02	0.01- 0.02	0.01- 0.02	0.02- 0.03	<i>b</i>	<i>b</i>	<i>b</i>
<a href="#">Figure 6.KB</a>	0.65- 0.6	<b>1.0+ -</b> 0.95	0.13- 0.12	< 0.1	0.14- 0.13	0.3- 0.2	< 0.1	< 0.1	< 0.1	<i>b</i>	<i>b</i>	<i>b</i>
<a href="#">Figure 7.KC</a>	<b>0.85-</b> <b>0.80</b>	0.65- 0.60	0.20- 0.19	0.18- 0.12	0.18- 0.12	0.09- 0.07	< 0.07	< 0.07	0.09- 0.08	<i>b</i>	<i>b</i>	<i>b</i>
<a href="#">Figure 8.To</a>	0.07- 0.06	0.09- 0.08	<b>0.5 -</b> <b>0.475</b>	<i>t</i>	<i>t</i>	<i>t</i>	< 0.06	< 0.06	< 0.06	<i>b</i>	<i>b</i>	<i>b</i>
<a href="#">Figure 9.Pu</a>	0.025- 0	0.025 -0	<i>b</i>	<i>t</i>	<i>t</i>	<i>t</i>	0.2	<b>0.35</b>	<i>t</i>	<i>b</i>	<i>b</i>	<i>b</i>
<a href="#">Figure 10.Ch</a>	0.05- 0.025	0.05- 0.025	0.075- 0.05	0.15- 0.125	0.175- 0.15	0.125 - 1.0	0.25-0	0.25-0	<b>0.25-</b> <b>0.225</b>	<i>b</i>	<i>b</i>	<i>b</i>
<a href="#">Figure 11.Ch</a>	0.175- 0.15	0.225- 0.2	0.175- 0.15	0.375- 0.35	0.375- 0.35	0.5	0.025- 0	0.025- 0	<b>1.0+</b> <b>-0.95</b>	<i>b</i>	<i>b</i>	<i>b</i>
<a href="#">Figure 12.Pe</a>	0.2- 0.175	0.25- 0.225	0.25- 0.225	0.3- 0.25	0.6- 0.55	> <b>2.0*</b>	0.15- 0.125	0.15- 0.125	0.15- 0.125	<i>b</i>	<i>b</i>	<i>b</i>
<a href="#">Figure 15.AI</a>	0.05- 0.025	0.075- 0.05	0.1- 0.075	0.1- 0.075	0.275- 0.25	0.1- 0.075	<i>b</i>	<i>b</i>	0.375- 0.35	<b>1.0+ -</b> <b>0.95</b>	0.475- 0.450	0.125- 0.1

Table A1: Modelling predicted maximum wave heights (in meters) likely to be detected at the DART tsunami buoys points in the open ocean (Locations of the buoys can be found in Figure 3). *b*= modelling boundary cuts off buoy. *t* indicates that the modelling was stopped before tsunami (of any height) is able to reach the buoy location. \*additional range from and extra resolution ran which is not shown in any of the figures.